High Quality factor photonic crystal nanobeam cavities

Parag B. Deotare, Murray W. McCutcheon, Ian W. Frank, Mughees Khan and Marko Lončar

School of Engineering and Applied Sciences, Harvard University, Cambridge, MA 02138

(Dated: February 5, 2009)

We investigate the design, fabrication and experimental characterization of high Quality factor photonic crystal nanobeam cavities in silicon. Using a five-hole tapered 1D photonic crystal mirror and precise control of the cavity length, we designed cavities with theoretical Quality factors as high as 1.4×10^7. By detecting the cross-polarized resonantly scattered light from a normally incident laser beam, we measure a Quality factor of nearly 7.5×10^5. The effect of cavity size on mode frequency and Quality factor was simulated and then verified experimentally.

For the past decade, there has been a concerted research effort to develop ultra-high Quality (Q) factor electromagnetic cavities with dimensions comparable to the wavelength of light [1, 2, 3, 4, 5, 6]. By shrinking the modal volume to near the fundamental limit of $V = (\lambda/2n)^3$, these cavities have enabled new applications to emerge in ultrasmall lasers [7, 8, 9, 10], strong light-matter coupling [11, 12, 13, 14, 15, 16], optical switching [17], and chemical sensing [18, 19], among others. Recently, there has been much interest in cavities realized in suspended nanobeams patterned with a one-dimensional (1D) lattice of holes [20, 21, 22, 23] due to their exceptional cavity figures of merit (Q and V), relative ease of design and fabrication, and potential for novel optomechanical effects [24, 25]. These apparently simple structures, which resemble very early microcavity prototypes [26], actually have Q/V factors which rival the best 2D planar photonic crystal cavities [3, 4]. They also have many inherent advantages, including the possibility of realizing high Q/V cavities in moderate index materials such as SiN_x [22] and facilitating coupling to ridge waveguides [21]. In addition, the near-field of the cavity is also highly "accessible", in the sense that there are two dimensions with total-internal-reflection (TIR) interfaces, which should facilitate bio-sensing applications as well as novel techniques for the dynamic control of cavity resonances [27].

In this paper we describe the design, fabrication, and experimental characterization of silicon photonic crystal nanobeam (PhCnB) cavities operating near ~ 1500 nm with measured Q factors of 7.5×10^5. To our knowledge, this represents the highest Q factor ever measured in nanocavities based on photonic crystal nanobeams, and one of the highest Qs ever measured in any photonic crystal cavity. Electromagnetic field confinement in the structure [Fig. 1(a)] is achieved by index guiding in two directions (y and z), and Bragg scattering from the 1D photonic crystal mirror in the third (x) direction. The mechanism of light confinement has been interpreted in terms of impedance matching [20, 22, 28] and the mode-gap effect [23]. Conceptually, the cavity can be viewed as a wavelength-scale Fabry-Perot cavity with photonic crystal mirrors which reflect and thus trap the nanobeam waveguide mode. Because the cavity mode penetrates some distance into the mirror, it is crucial that the fields do not abruptly terminate at the mirror boundary, as this would lead to considerable scattering loss [28]. To avoid this impedance mismatch between the

waveguide mode and the Bloch mode, the photonic crystal mirror is tapered by reducing the hole spacing (a) and radius to match the effective indices of the evanescent mirror Bloch mode, $n_{Bl} = \lambda/2a$, and the waveguide mode, $n_{wg} = 2.41$. The cavities were designed using the 3D finite-difference time-domain (FDTD) method (Lumerical Solutions, Inc.) and incorporate a five-hole linear taper in a free-standing silicon nanobeam of thickness 220 nm (constrained by our experimental wafer) and width 500 nm, as detailed in Fig. 1. With the tapered mirrors designed to minimize reflection loss from the incident lowest-order waveguide mode, the cavity length is scanned to optimize the Quality factor of the fundamental cavity mode, as shown in Fig. 3(c). The Q factor is calculated from the definition: $Q = \omega_0 \frac{\text{Energy stored}}{\text{Power loss}}$, and is validated in the lower Q structures by monitoring the time-domain ring-down of the fields. The optimal structure supports a fundamental mode at $\lambda = 1560$ nm with a Q factor of 1.4×10^7 and an ultra-small mode volume of $V = 0.39 \ (\lambda/n)^3$. The mode profile is plotted in Fig. 1(a). The cavity also supports higher-order modes with different symmetry, one of which is shown in Fig. 1(b), and which has a reasonable Q factor of 120,000 and mode volume $V = 0.71 \ (\lambda/n)^3$.

The devices were fabricated on a silicon-on-insulator (SOI) substrate (SOITEC Inc) with a device layer of 220nm and an insulator layer of 2 μm. A negative electron-beam (e-beam) lithography resist, Foxx-17 (Dow
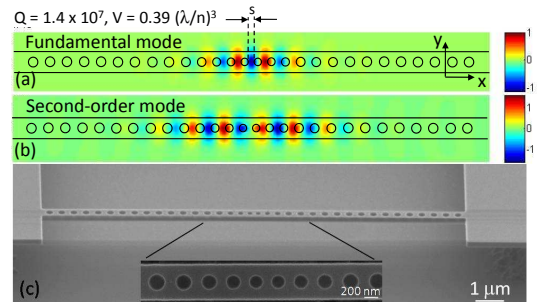

FIG. 1: (a,b) Electric field (E_y) profiles of the two cavity modes. Q and V are quoted for the optimal cavity length, s. (c) SEM image of a fabricated photonic crystal nanobeam cavity. The nanobeam thickness is 220 nm and width is 500 nm. The photonic mirror pitch $a = 430$ nm is linearly tapered over a 5 hole section to $a = 330$ nm at the cavity center. The hole radius is given by r = 0.28a. The 1D photonic bandgap extends from 1200-1700 nm.

Corning) diluted in Anisole in a 1:6 ratio, was used for e-beam lithography. The film was spin coated onto the sample at 5000 rpm and then baked at 90°C on a hot plate for 5 minutes, resulting in a total film thickness of 135 nm. Patterns were defined using a standard 100kV e-beam lithography tool (Elionix) and developed in tetramethyl ammonium hydroxide (25% TMAH) followed by a thorough DI water rinse. The devices were etched in a reactive ion etcher (STS-ICP RIE) using SF_6, C_4F_8 and H_2 gases. Removal of the oxide sacrificial layer was carried out using a HF vapor etching (HFVE) tool (AMMT) operating at 35°C, which resulted in an etch rate of approximately 125 nm/min [29]. This technique produced more reliable results than the more conventional approach of a wet etch followed by critical point drying. A complete fabricated device is shown in Fig. 1(c). A number of photonic crystal cavities were made by systematically varying the cavity length (s), resulting in resonators with different Quality factors and operating wavelengths.

The fabricated devices were tested using a resonant scattering optical setup [30, 31] (Fig. 2). Prior to entering the objective lens, the polarization of the incident laser beam is rotated by 45° using a half-wave plate (HWP), so that the E-field of the focused laser spot and the major component of the cavity mode (E_y) form a 45° angle. Light coupled in and subsequently re-emitted (back-scattered) by the cavity is collected using the same objective lens, and then its polarization is rotated by -45° after passing through the same HWP. The back-scattered signal is then split using a beam splitter (BS), analyzed using a polarizer (P2) that is cross-polarized with respect to the polarization of the incoming laser beam, and finally detected using an InGaAs detector. This combination of polarizers and wave plates enhances the ratio between the resonantly scattered signal from the cavity and the coherent background due to non-resonant reflections. The spectra are normalized by a non-resonant background taken away from the cavity. Because of the coherent relationship between the scattered signal and the background, resonances appear as dips or peaks (depending on the geometry) and can have an asymmetric shape similar to Fano resonances. In this scheme, the cavity plays the role of a wavelength selective polarization rotator. Our experimental approach therefore allows for resonant spectroscopy of the cavity, and does not require integration of additional waveguides to couple light in and out of the cavity. Therefore, our method measures the intrinsic Q factor of the cavity without "loading" effects due to the presence of coupling waveguides.
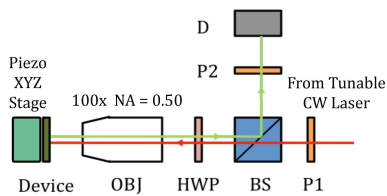

FIG. 2: Schematic of experimental set-up (OBJ: microscope objective, HWP: half-wave plate, BS: beamsplitter, P1 and P2: polarizers, D: detector).
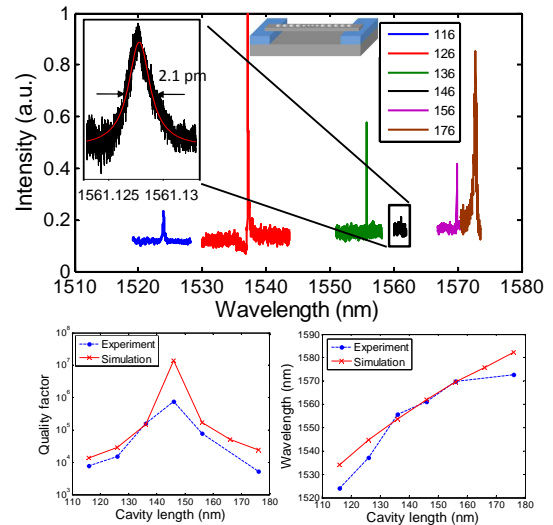

FIG. 3: (a) Resonant scattering spectra for a range of cavities (s = 116-176 nm) normalized by a background spectrum taken on the beam away from the cavity. (b) Measured and simulated Quality (Q) factors as a function of cavity length (s).(c) Mode resonance wavelength as a function of s.

The experimental results are shown in Fig. 3. We expect that as the cavity becomes longer, the resonance should redshift due to the increase in the effective index of the cavity. This behavior is well modelled by our simulations, and we see a similar overall trend in our experimental results. Detailed investigation of fabricated structures using scanning electron microscopy (SEM) revealed that deviations from theoretical results can be attributed to fabrication-related disorders, and in particular to proximity effects during e-beam lithography. The cavity Q factor also follows the predicted trend. As expected, for large and small s, the Q factor is modest ($Q < 10,000$), and it reaches a record high value of $Q = 750,000$ when $s = 146$ nm. We also found that the cavity resonance was very sensitive to the excitation location, and disappeared with sub-micron displacements of the cavity. This is consistent with the expected small mode volume of our cavities.

We fabricated a range of structures with scaled dimensions to account for imperfections introduced during fabrication and to effectively bracket the design parameters. We found that the structures scaled by -3% most closely matched our simulations, and the spectra from these cavities are the ones presented in Fig. 2. It is interesting to note that cavities with a higher Q factor were more difficult to characterize using our resonant scattering setup, and had a reduced contrast between the resonant feature and the coherent non-resonant background. This may be an intrinsic property and fundamental limitation of the resonant scattering approach, and it will be addressed in our future publications.

We also tested our nano-beam resonators before the final release HFVE step. Non-suspended, on-substrate cavities are more robust and are suitable for such applications as sensing and operation in fluids [19]. Fig. 4 shows the experimental results for several resonator de-
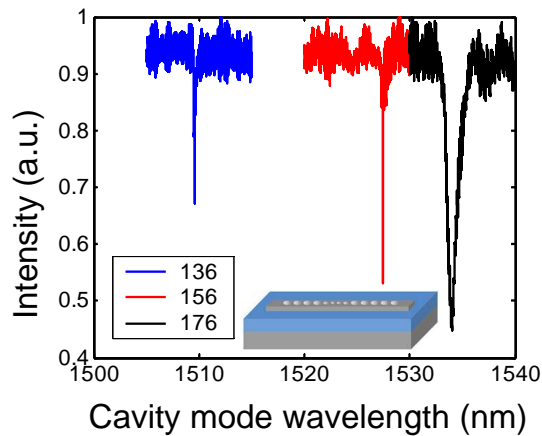
FIG. 4: Resonant scattering spectra for on-substrate SOI cavities (not undercut). The Q factors are 18,000; 27,500; and 17,000 for the $s = 136$, 156, and 176 nm cavities, respectively.

signs with varying cavity spacing, s, taken before the cavities were released from the substrate. The highest Q factor that we were able to obtain was 27,500 for a cavity with $s = 156$ nm. Higher Q factor results have been previously reported in different on-substrate PhCnB cavities [21]. We note, however, that our cavities were optimized for free-standing operation, and therefore the modest Q factors are not surprising.

In conclusion, we have successfully designed and fabricated ultra high-Q photonic crystal nanobeam cavities using our novel five-hole taper design with a measured Q factor of 7.5×10^5. The devices on silicon dioxide have also been studied and show a moderate Q factor, on the order of 10^4. We have also reported, for the first time, the successful use of the resonant scattering method for measuring photonic crystal nanobeam cavities.

[1] O. Painter, J. Vučković, and A. Scherer, J. Opt. Soc. Am. B **16**, 275 (1999).
[2] Y. Akahane, T. Asano, B. S. Song, and S. Noda, Nature **425**, 944 (2003).
[3] B. S. Song, S. Noda, T. Asano, and Y. Akahane, Nature Materials **4**, 207 (2005).
[4] E. Kuramochi, M. Notomi, S. Mitsugi, A. Shinya, T. Tanabe, and T. Watanabe, Appl. Phys. Lett. **88**, 041112 (2006).
[5] K. Srinivasan, P. E. Barclay, and O. Painter, Opt. Express **12**, 1458 (2004).
[6] J. Topolancik, F. Vollmer, and B. Ilic, Appl. Phys. Lett. **91**, 201102 (2007).
[7] O. Painter, R. K. Lee, A. Scherer, A. Yariv, J. D. O'Brien, P. D. Dapkus, and I. Kim, Science **284**, 1819 (1999).
[8] M. Loncar, T. Yoshie, A. Scherer, P. Gogna, and Y. M. Qiu, Appl. Phys. Lett. **81**, 2680 (2002).
[9] K. Nozaki, S. Kita, and T. Baba, Opt. Express **15**, 7506 (2007).
[10] H.-G. Park, S.-H. Kim, S.-H. Kwon, Y.-G. Ju, J.-K. Yang, J.-H. Baek, S.-B. Kim, and Y.-H. Lee, Science **305**, 1444 (2004).
[11] T. Yoshie, A. Scherer, J. Hendrickson, G. Khitrova, H. M. Gibbs, G. Rupper, C. Ell, O. B. Shchekin, and D. G. Deppe, Nature **432**, 200 (2004).
[12] J. P. Reithmaier, G. Sek, A. Loffler, C. Hofmann, S. Kuhn, S. Reitzenstein, L. V. Keldysh, V. D. Kulakovskii, T. L. Reinecke, and A. Forchel, Nature **432**, 197 (2004).
[13] K. Hennessy, A. Badolato, M. Winger, D. Gerace, M. Atature, S. Gulde, S. Falt, E. L. Hu, and A. Imamoglu, Nature **445**, 896 (2007).
[14] D. Englund, A. Faraon, I. Fushman, N. Stoltz, P. Petroff, and J. Vučković, Nature **450**, 857 (2007).
[15] K. Srinivasan and O. Painter, Nature **450**, 862 (2007).
[16] J. Vučković, M. Lončar, H. Mabuchi, and A. Scherer, Phys. Rev. E **65**, 016608 (2001).
[17] T. Tanabe, M. Notomi, S. Mitsugi, A. Shinya, and E. Kuramochi, Appl. Phys. Lett. **87**, 151112 (2005).
[18] M. Lončar, A. . Scherer, and Y. Qiu, Appl. Phys. Lett. **82**, 4648 (2003).
[19] D. Erickson, S. Mandal, A. H. J. Yang, and B. Cordovez, Microfluidics and Nanofluidics **4**, 33 (2008).
[20] C. Sauvan, G. Lecamp, P. Lalanne, and J. Hugonin, Opt. Express **13**, 245 (2005).
[21] A. R. M. Zain, N. P. Johnson, M. Sorel, and R. M. D. la Rue, Opt. Express **16**, 12084 (2008).
[22] M. W. McCutcheon and M. Lončar, Opt. Express **16**, 19136 (2008).
[23] M. Notomi, E. Kuramochi, and H. Taniyama, Opt. Express **16**, 11095 (2008).
[24] M. L. Povinelli, M. Loncar, M. Ibanescu, E. J. Smythe, S. G. Johnson, F. Capasso, and J. D. Joannopoulos, Opt. Lett. **30**, 3042 (2005).
[25] M. Eichenfield, R. Camacho, J. Chan, K. J. Vahala, and O. Painter, arXiv:0812.2953v1 [physics.optics] (2008).
[26] J. S. Foresi, P. R. Villeneuve, J. Ferrera, E. R. Thoen, G. Steinmeyer, S. Fan, J. D. Joannopoulos, L. C. Kimerling, H. I. Smith, and E. P. Ippen, Nature **390**, 143 (1997).
[27] A. F. Koenderink, M. Kafesaki, B. C. Buchler, and V. Sandoghdar, Phys. Rev. Lett. **95**, 153904 (2005).
[28] P. Lalanne and J. P. Hugonin, IEEE J. Quantum Electron. **39**, 1430 (2003).
[29] P. B. Deotare, M. Khan, and M. Loncar, Proc. SPIE **7205**, 720509 (2009).
[30] M. W. McCutcheon, G. W. Rieger, I. W. Cheung, J. F. Young, D. Dalacu, S. Frédérick, P. J. Poole, G. C. Aers, and R. L. Williams, Appl. Phys. Lett. **87**, 221110 (2005).
[31] K. Rivoire, A. Faraon, and J. Vučković, Appl. Phys. Lett. **93**, 063103 (2008).